Engineering geology study of Lingquansi Cave Temple, People's Republic of China

He Yan · Li Zhiyi · Yang Zhifa · Wang Jianfeng

Abstract The Lingquansi Cave Temple, in the Henan Province of China, is a cultural heritage relic of national importance. Exquisitely cut in the rock mass, the images of Buddha in low relief, the inscriptions and the Buddhist scriptures are all stone carving art treasures of the Sui Dynasty. The cave temple was constructed on intact and compacted crystalline limestone between the fifth and tenth centuries A.R. Heavy geological deterioration and other factors have resulted in various degrees of damage to the temple's grottoes and stone carvings over the centuries such that protection and renovation are urgently required. Dazhu Grotto and the biggest and best stone carvings are the main concerns of the engineering geological study discussed here. Detailed investigations of the nature of deterioration have been carried out and proposals for remedial/preservation works are presented.

Résumé Le temple de Lingquansi Cave, dans la province de Henan (Chine), constitue un héritage culturel d'importance nationale. Sculptées avec finesse dans la masse rocheuse, les images de Bouddha en bas-relief, les inscriptions et écritures bouddhiques sont des trésors artistiques de la dynastie Sui. Le temple-grotte fut construit sur des calcaires cristallins compacts entre le cinquième et le dixième siècle a.d. Au cours des siècles, l'altération géologique et d'autres facteurs ont conduit à divers dommages affectant les grottes du temple et les sculptures, de sorte qu'une protection et une rénovation sont devenues urgentes. La grotte Dazhu ainsi que la plus belle et plus grande sculpture sont les principaux objets d'étude géologique de cet article. Des recherches détaillées sur la nature des détériorations ont été réalisées et des propositions de travaux de rénovation et préservation sont faites.

Keywords Cave temple · Grotto · Environment · Geological deterioration · Renovation · China

Mots clés Temple · Grotte · Environnement · Altération géologique · Rénovation · Chine

Received: 15 January 2000 · Accepted: 29 August 2000

He Yan (✉) · Yang Zhifa
Engineering Geo-mechanics Open Research Laboratory,
Institution of Geology and Geophysics,
Chinese Academy of Sciences, 100029 Beijing,
People's Republic of China
e-mail: zhuzl@263.net or zhuzl@chinaren.com
Tel.: +86-10-62008075
Fax: +86-10-62040574

Li Zhiyi
College of Engineering Technology, China University of Geo-sciences, 100083 Beijing, People's Republic of China

Wang Jianfeng
Non-linear Mechanism Open Research Laboratory, Institution of Mechanism, Chinese Academy of Sciences, 100022 Beijing, People's Republic of China

Introduction

The Lingquansi Cave Temple in the Taihang Mountains is located about 30 km southwest of Anyang City in Henan Province, central China (Fig. 1). The 1,450-year-old temple was established during the Northern and Southern Dynasties when Buddhism was flourishing in the region. At that time it was best known as "The first ancient temple in the HeShuo area" (Anon 1991). The temple site comprises the base of the temple itself, which has been ruined through the course of history, and a plenitude of niches for statues of Buddha located on escarpments of the adjacent Bao and Lanfeng Mountains to the west and east of the original temple. In total there are 209 niches, 153 of which are cut on escarpments and 75 of which are engraved with inscriptions. There are also two large rock caves; the larger Dazhu Grotto in the Bao Mountain and the smaller Daliu Grotto in the Lanfeng Mountain.

There are 120 niches (numbered K1–K120) in the rock mass on the southern slope of the Bao Mountain, about 0.5 km from the western side of the temple base. The total length of the niche area is 520 m and the height over the

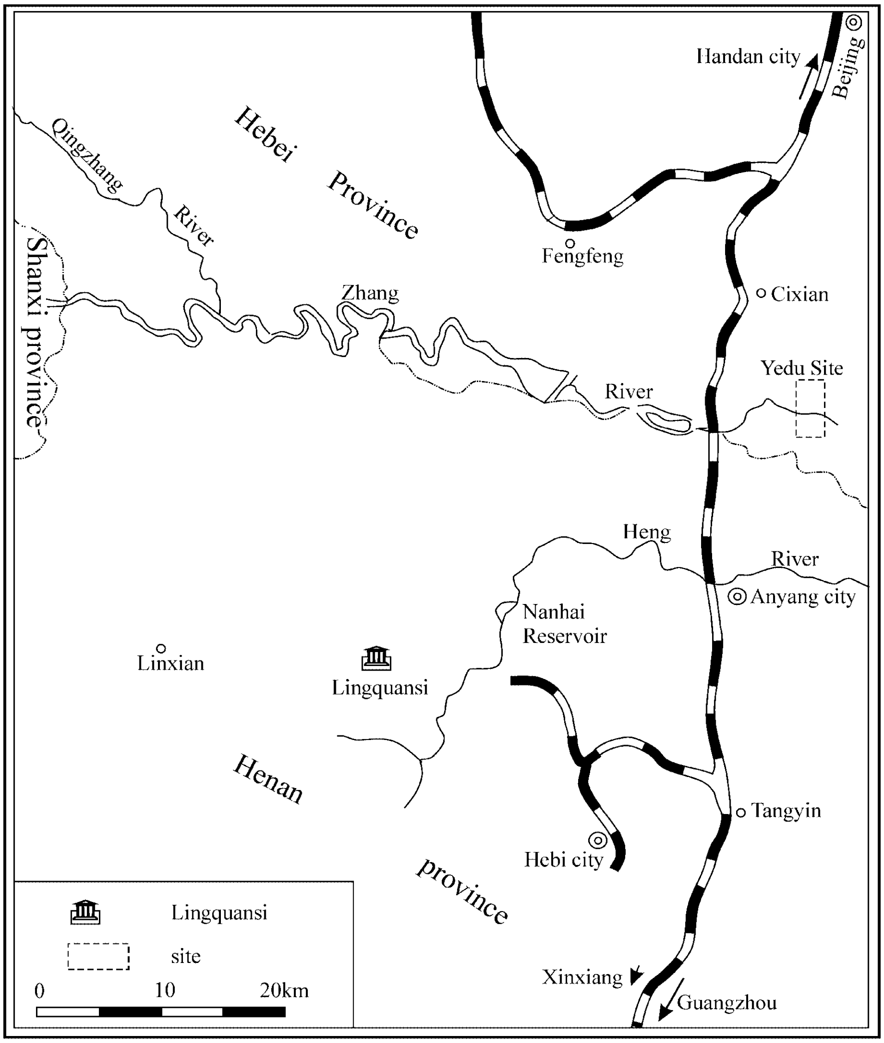

Fig. 1
Location of study area

valley floor varies from 38–67 m. In accordance with the shape of the escarpment, the niches are arranged in top, middle and bottom layers in seven sub-areas (W1–W7). The remainder (numbered K121–K209) are located on the rock mass of the western foot of the Lanfeng Mountain, about 1 km northeast of the temple. The total length of this niche area is 310 m and the height above the valley floor is between 43 and 60 m.

The stone carvings and inscriptions, on a grand scale, constitute precious historical materials for the study of architecture, engraving, religion, dance, calligraphy, art, etc. However, over the centuries the Lingquansi Cave Temple has developed serious structural problems, both from natural causes and as a result of man's activity. These include instability of the rock escarpment, water percolation and corrosion and weathering. This has resulted in different types of damage and the stone carvings are now in need of immediate renovation and protection.

The Dazho Grotto, the stone carvings and the inscriptions on the Bao Mountain escarpment are, on the whole, relatively better preserved and have a higher cultural relic value than those on the Lanfeng Mountain escarpment. For these reasons they have been selected for the study presented in this paper, the purpose of which was to undertake an engineering geological analysis as a basis for determining the most appropriate renovation and protection methods. As seismicity is an important trigger for sliding or collapse and the Lingquansi Cave Temple requires long-term protection, it was decided to: (1) analyse and numerically simulate the deformation of the particular slope where the Dazhu Grotto and the stone carvings K1–K120 are located; (2) determine the reasons for the slope deformation and failure and the laws of their development; and (3) predict, through specific studies of the slope, potential deformation and failure of the slope under future seismic action.

In the analyses, the following terminology has been adopted: the cave temple denotes the whole temple complex in the study area, including all stone carvings and inscriptions, as well as both grottoes; stone carvings denote niches and inscriptions present on the southern escarpment of the Bao Mountain; and the grotto denotes the Dazhu Grotto including some stone carvings and inscriptions located both outside and inside the cavern.

Geological setting

Basic engineering geology conditions

In the study area the eastern extension of the Taihang Mountains consists of 300- to 500-m-high hills such as the Bao Mountain and the Lanfeng Mountain as shown in Fig. 2. The dominant geology is the carbonate rock of the Majiagou Formation, part of the Lower Ordovician system. Diorites intruded into these Lower Palaeozoic rocks. Quaternary sediments of different genesis are present in the intermontane basin and on both sides of the valley. The carbonate rock comprises crystalline limestone and dolomitic limestone. Where the limestone was in contact with diorite, pyromorphism has resulted in the formation of marble. The grotto and the stone carvings were created only on the crystalline limestone and marble.

In terms of the geomechanics of the region, the convergence between the first-order Taihang Mountain systems uplift in the west and the North China sag of the Neocathaysian structural systems to the east is marked by the intersecting Anyang–Handan fault zone. The dominant regional tectonic direction is north–northeast and gently dipping monoclinal structures are the master structural types. The Anyang–Handan fault zone, which runs approximately parallel to the BeiJing–Guangzhou Railway to the east (Fig. 1), is composed of many fractures and affects crust stability.

Two groundwater aquifers are found in the region: in the karst bedrock fissures and in the loose sediments. The former is buried in the fissures of the carbonate rocks at greater depths, while the latter is a phreatic aquifer located in the Quaternary sandy pebble bed.

Table 1
Recorded earthquakes with magnitudes >5 (Richter) registered in the Lingquansi Cave Temple study area

No.	Date	Epicentre location	Magnitude
1	4/10/1587	Northwest of Weihui	6
2	2/4/1814	Between Tangyin and Junxian	5.5
3	5/1829	Southeast of Hebi	5.25
4	6/12/1830	Cixian	7.5
5	5/1900	West of Anyang	5
6	8/2/1980	Linzhou	5.1

Seismicity

According to historical records, a number of earthquakes have occurred in the area surrounding the cave temple, six of which registered as greater than 5.0 on the Richter scale (Table 1). The strongest registered earthquake, which occurred in 1830 with an epicenter at Cixian, had a magnitude of 7.5. The isoseismal lines for this quake are shown in Fig. 3. This earthquake caused damage to the study area

Fig. 2
Environmental geology map for Lingquansi Cave Temple

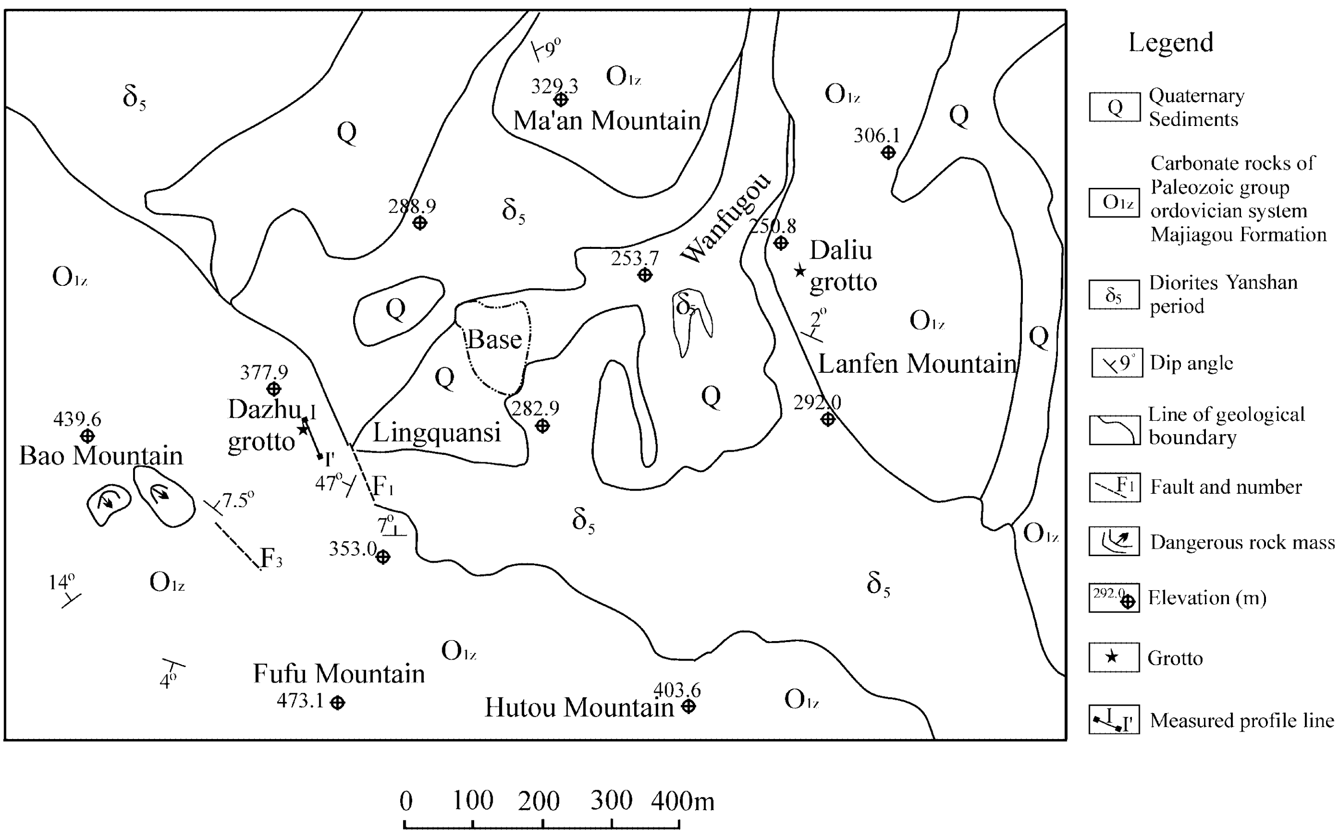

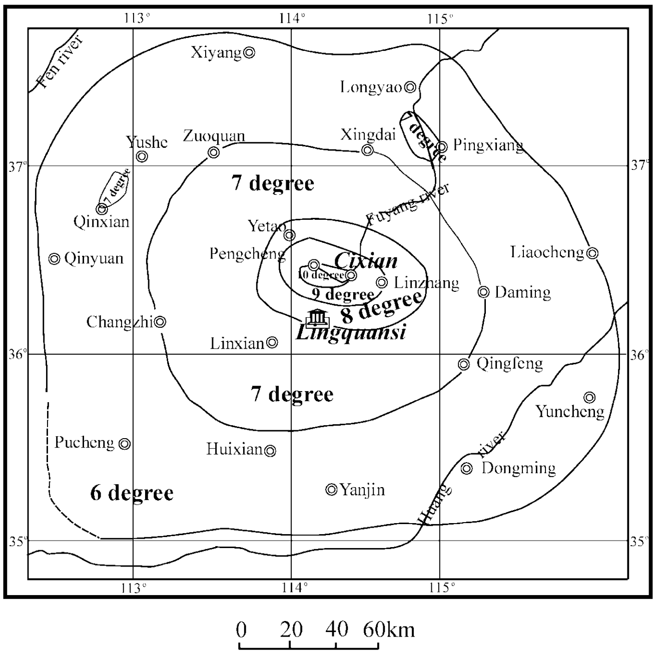

Fig. 3
Isoseismal lines for the 1830 Cixian Earthquake with magnitude 7.5 (Richter)

Fig. 4
Three disturbed blocks in Lingquansi Cave Temple study area

at a level of 8 degrees on the earthquake intensity scale. Bearing in mind the relatively young and strong tectonic activity in the region, it can be assumed that the study area is located in a high-intensity seismic region.

From field studies it appears that the dislocations of rock blocks, dissected by many sets of structural planes, are mainly associated with earthquakes. To the east of the grotto door, for example, the rock has clearly moved towards the free face and now forms a dangerous rock mass comprising of three disconnected blocks overlapping one another (Fig. 4). From top to bottom the blocks have moved by some 200–300, 100–200 and 50–100 mm respectively. Similar features occur in the rock mass to the west. The seismic influence on the stability of the blocks, especially the already dangerous rock blocks, is therefore an important factor to take into account in the prevention and control of geological disturbances and decay.

Rock mass characteristics of the cave temple

The lithological composition of the carbonate rock mass is predominantly crystalline limestone, marble and crystalline limestone with a granophyric texture. Intact, dark grey, thickly bedded crystalline limestone forms the base, while light grey and massive thickly bedded crystalline limestone with a granophyric texture forms the steeper slope of escarpment. Karst features such as karren, solution grooves and solution holes are well developed along bedding planes and joints in both strata (Fig. 5). Milky white and massive thickly bedded marble evidences the thermal metamorphism of the crystalline limestone. Resistance to weathering is strong.

Rock mass structure

As structural planes of different scales have varying degrees of influence on the stability of the rock mass, it was necessary to carry out studies to determine the extent of the structural planes and their effect on rock mass stability. According to the grading of structural planes proposed by Gu Dezhen (1979a), fourth-order structural planes in carbonate rocks are relatively narrow and are of limited length both along the strike and in depth.

In the study area, fourth-order structural planes of different scale and direction are seen as steeply dipping joints. The bedding plane dips gently towards the mountain interior at an angle of 4–14° and is favourable to the overall stability of the slope. However, the dissections of

Fig. 5
Solution grooves well developed along bedding planes and joints in thickly bedded crystalline limestone

the fourth-order structural planes and bedding planes directly affect not only the mechanical properties and stress distribution but also, to some degree, the failure patterns of the rock mass. The pull-apart of the fourth-order structural planes is regarded as the most important inducing factor in geological deterioration.

A total of four sets of structural planes, identified as J_1, J_2, J_3 and S_0, have been measured, with orientations and declinations of 68° at 074°N, 82° at 146°N, 63° at 255°N and 6° at 314°N respectively. A probability statistical analysis of their geometric parameters demonstrates that the rock mass has comparatively good integrity and clear anisotropy in sectional view. The major directions of water flow are nearly vertical, following the inclination of the bedding planes.

Engineering geological field investigations and research by the authors indicates that according to Gu Dezhen's (1979b) classification of the general structure types of rock masses, the rock mass of the cave temple has a block structure pattern. The rock mass is dissected into rectangular, columnar, cubic or rhombic blocks with an average volume of about 1 m^3 by two or three sets of principal fourth-order structural planes. There are many sets of fractures with relatively good continuities within the rock mass and this is evidence of groundwater movement.

The mode of failure or deformation of a rock mass is largely controlled by its structure. In a rock mass with a block structure, blocks are likely to slide or pull-apart along structural planes – an important consideration when preparing recommendations or engineering geological plans for the renovation of the cave temple.

Physical/mechanical properties of the rock

The rock studied here is pure limestone. As confirmed through X-ray diffraction analyses (XRD), the principal chemical composition of fresh samples of the crystalline limestone and marble is calcium oxide (CaO), with minor amounts of carbon dioxide (CO_2) also present. The scanning electron microscope (SEM) showed a mineralogical composition of crystalline limestone consisting almost entirely of calcite, with three sets of cleavage planes and local corrosion marks clearly seen. Primary pores among the crystal grains, along which groundwater can percolate, confirmed the possible development of karst under certain conditions.

The results of the Schmidt rebound hammer test are shown in Table 2. The data indicate that the rock materials of the grotto and the stone carvings have the following characteristics: (1) the rock of the inner grotto has a higher mechanical strength than the same rock in the external grotto. The uniaxial compressive strengths were generally over 100 MPa, with a maximum value of 152 MPa. As would be expected, this indicates that weathering is a main factor affecting the mechanical strength of the rock; (2) the integrity of the rock mass decreases and mechanical strengths are low where there is a dual effect of the intersection of structural planes and the weathering of the rock mass.

Detrimental geological phenomena

The main geological hazards in these rocks are collapse and karstic features. As a consequence of the steep landform and the development of two or three sets of steeply dipping joints, fissures are generated in the near-surface rock mass of the slope, under gravity and in order to relieve loading stresses. As a result, the stability and the integrity of the stone carvings are reduced. Karst develops mainly in the limestone and appears principally as vertical solution along fissures, solution hollows and small caves originating along bedding planes. In addition to their effect on the stability of the stone carvings, percolating water and corrosion along fissures or bedding planes results in the deposition of sediments on the surface, reducing both the clarity and aesthetic appearance of the stone carvings and inscriptions.

Table 2
Uniaxial compressive strengths for the Dazhu Grotto obtained by correlation with Schmidt hammer rebound numbers. Lithology is crystalline limestone (especially marble in W5) and direction is horizontal in the entire test

Test location	Rock density ρ (g/cm^3)	Conversion uniaxial compressive strength σ_c (MPa)	Mean uniaxial compressive strength σ_c (MPa)
Western wall rock	2.70	40	102
Eastern wall rock	2.70	84	
Base of western niches	2.77	152	
Base of eastern niches	2.77	130	
Stone carving in W2	2.73	63	
Stone carving in W3	2.57	50	
Stone carving in W5	2.69	42	

Geological analyses of the grotto and stone carvings

As a result of the different environments that affect the grotto and stone carvings, there are differences in the deformation, failure patterns and geological changes they experience. These are discussed separately below.

Types of geological deterioration of the grotto

The uniaxial compressive strength of the grotto's crystalline limestone is, on average, up to 102 MPa (Table 2). Despite their age of over 1,450 years, the stone carvings inside the grotto are basically unweathered and not corroded. The principal problems are deformation of the rock wall, water percolation and corrosion as well as the deposition of carbonate sediments on the surfaces (dripstone).

Figures 6 and 7 show the results of the examination of the door to the Dazhu Grotto and the stone carvings inside the grotto respectively. The strata dip 6–8° in the directions 85–115°N. The structure of the rock, dipping gently towards the interior of the mountain, aids the stability of the escarpment. However, there is evidence of the development of a solution hole as a result of water percolation along pull-apart bedding-plane fissures on the bottom of the eastern, northern and western sides of niches for statues of Buddha inside the grotto. In the rock mass at the bottom of the grotto, weathering of a weak, thinly bedded muddy intercalation has resulted in a hollow some 100 mm high. This will clearly influence the stability of the grotto. In addition, there are two orthogonal sets of steeply dipping joints. The first, J_1 (85°/015°N), transects the top, eastern and western sides of the grotto and has been pulled apart into a 2 mm wide fissure along which water can percolate during periods of rain. J_2 (74°/100°N) crosses the middle part of the grotto ceiling and branches on the northern side of the grotto. Again, this provides a passageway for percolating water, which exacerbates the opening of the joint. The fissure crosses the central part of two guards in relief on the surface of the grotto door, forming a crack up to 5 mm wide.

It is very clear that the dissection of the three sets of structural planes must affect the integrity of the rock, while their opening dominates both the stability of the wall and the damage to its surface.

As a result of water percolating through the fissures, there are many wet areas on both the grotto ceiling and the northern side of the niche. In addition, a pervasive calcareous tuff now covers part of the figures of Buddha and the inscriptions, while all the heads and most of the hands of the images of Buddha exhibit varying degrees of man-made damage.

Types of geological deterioration of the stone carvings

The stone carvings are subject to atmospheric weathering, with the result that fractures have developed and the strength of the rock mass and its capacity to resist further weathering has been reduced. The degree of stability of the rock mass is inseparably connected with the various dissections of the structural planes and the free faces.

In the area of niches K75 and K76 of W3, a dangerous rock block (Fig. 8) some $1.5 \times 1.2 \times 1.5$ m has been created by the intersection of bedding-planes and two sets of steeply dipping joints (81°/010°N and 88°/240°N respectively). This block has clearly moved towards the free face and there are other dangerous rock masses on its eastern side.

At the bottom of some of the stone carvings in the location of W5, weathering of a weak thinly bedded intercalation of impure dolomitized limestone has resulted in the formation of hollows up to 300 mm high and 0.3–1 m deep. As a consequence, some of the stone carvings have lost their support and are now hanging freely. In addition, there are two sets of steeply dipping joints with declinations of 88°/185°N and 82°/065°N respectively. Where they intersect the bedding planes, this adds to the instability of the rock mass and one of the stone carvings has already collapsed.

At the same time, networks of water percolation channels have formed where structural planes intersect and karst phenomena, including solution channels and hollows, are common along the bedding planes. Indeed, in parts of the stone carvings in W2 and W3, such cracks and holes may be as deep as 10 mm. They are often infilled with a calcareous cement, while a grey–white calcareous sediment partially obscures the carvings.

Weathering and denudation of the stone carvings are marked. The biggest niche, K70 in W3, is a typical example. The lower part of this niche is in crystalline limestone with little resistance to weathering. Exfoliation has occurred on the surface and the inscriptions are difficult to distinguish (Fig. 9). Fortunately, the upper part of the niche is in marble and here the inscriptions can still be identified.

Analysis of geological problems

The research carried out in the grotto and on the stone carvings indicates that, apart from man-made damage, the main problems result from instability of the rock mass on the escarpment, water percolation and weathering. Of these, the rock mass instability is considered most important. Physical weathering along the discontinuities results in a reduction in the strength and overall integrity of the rock, which is very detrimental to the stone carvings (Beitong and Kezhong 1992).

Rock mass instability

Intersecting structural planes are important factors in the deformation/failure of the grotto and the stone carvings. Several sets of fourth-order structural planes in the carbonate rock are relatively continuous and have dissected the rock mass into blocks of different shapes and sizes. The main pattern of instability is on the relatively steep free face, where blocks separated by the intersecting joints are most likely to deform or suffer gravity failure, either as a result of a buildup of pore-water pressures or as a consequence of earthquake forces.

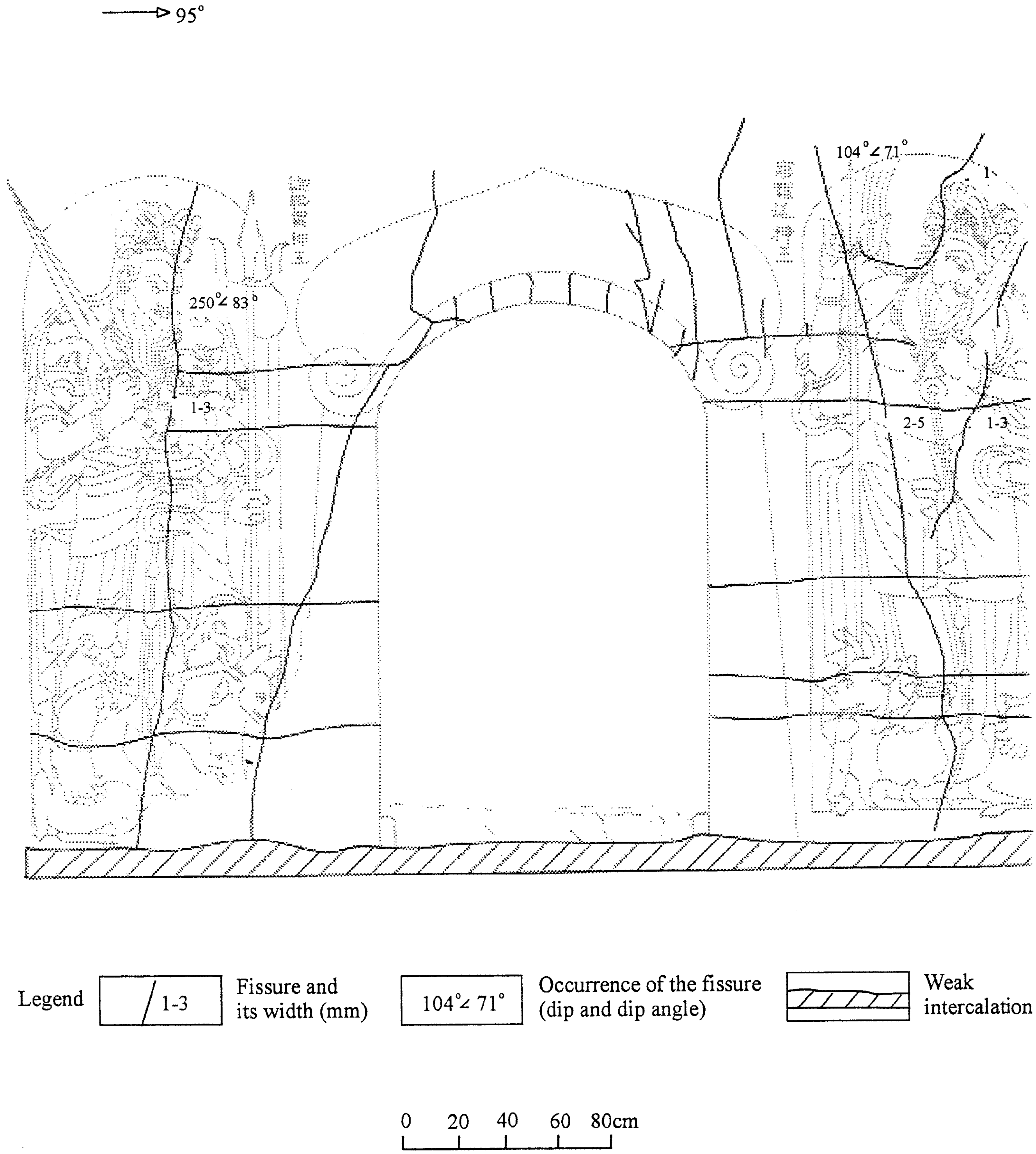

Fig. 6
Images of Buddha in relief at entrance of Dazhu Grotto

Water percolation and corrosion

The principal mineral composition in the limestone is calcite, which has a strong corrosion capacity. With a continuous natural recharge, there is sufficient carbon dioxide in the water for constant corrosion. To some extent this is controlled by the rock mass structure, hence water percolation and corrosion usually take place along structural planes. Such initial dissolution gradually leads to the formation of solution holes or karst caves, aided by the interconnection of micro-fractures in the crystalline limestone that has a granophyric texture and facilitates groundwater flow. These networks of weak structural planes, joints and fissures not only provide channels for water percolation and corrosion but also allow other

Fig. 7
Exposition of Dazhu Grotto

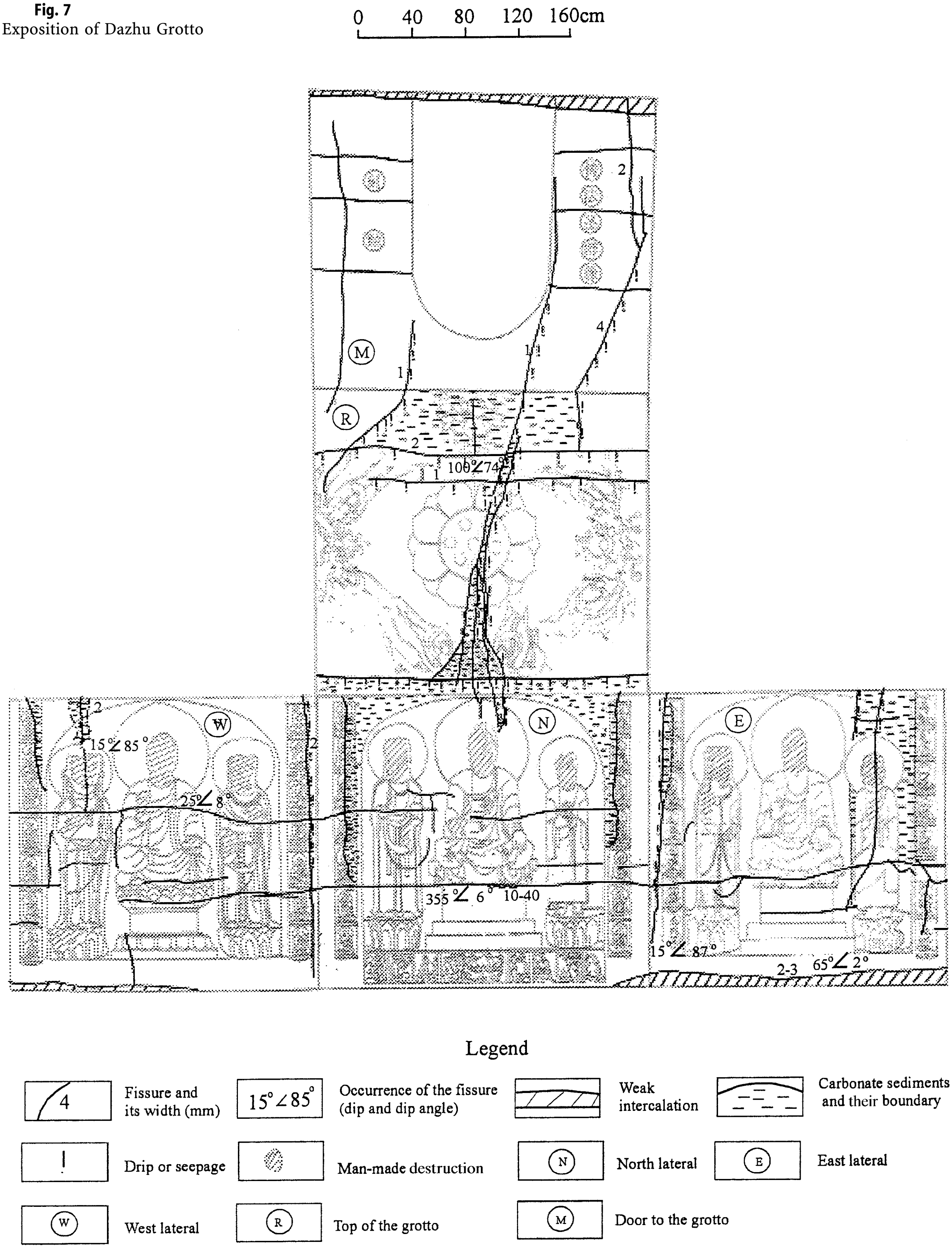

Fig. 8
Dangerous rock block in area of niches K75 and K76 of W3

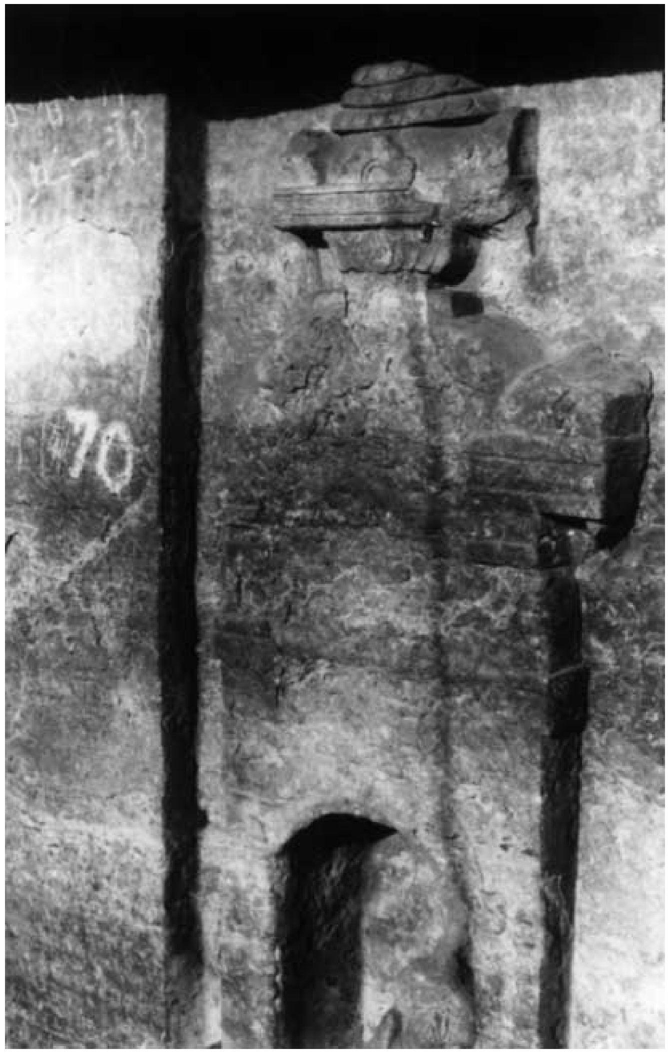

Fig. 9
Exfoliation on surface of niche K70 in W3

weathering agents such as air and rainwater to extend further into the rock mass in which the grotto and stone carvings have been created.

Rock mass stability analysis

Stability of the slope

Displacement field and stress field data can be obtained using the finite element method (FEM) which provides information for a slope stability analysis and subsequent remedial measures. In view of its composition and complicated structure, it is difficult to define the detailed properties of the rock mass precisely. A solution to this problem is an integrated experimental and theoretical method under various conditions and a simplified geological model to predict deformation of the slope based on geological data (XinPu et al. 1995).

Model establishment

In view of the cultural value of the stone carvings, a typical profile (I-I′) was selected and measured for analysis, as shown in Fig. 10. The profile consists of marble and crystalline limestone. A total of 401 elements with 407 nodal points were used, after discretization along bedding planes (Fig. 11). The nodal point displacements at the bottom boundary are assumed as zero in X and Y the direction i.e., bidirectional restrictions and the nodal point displacements at the left boundary (Y axis) are zero in the direction of X (Beitong and Runqiu 1994).
The elastic and plastic Drucker-Prager yielding criterion was adopted in the calculations. Only gravity and earthquake forces were considered; as the slope is releasing stress at present and the groundwater table is at some depth, it was not considered necessary to take earth stress and groundwater factors into account.

Selection of calculation parameters

For crystalline limestone and marble, the physical parameters were based on the Schmidt rebound hammer test results (Table 2) and on empirical data for rock mechanics as used in water conservation construction projects. In order to justify the parameters, back analyses were performed using the FEMA.FOR computer program (Yunfei and Jing 1992). Corresponding parameters meeting the requirement of a measured displacement value of 50–250 mm were calculated. The results are presented in Table 3.

Stability calculation and evaluation

In this analysis, a local stability evaluation method (Handong 1997) was adopted based on stress data obtained from the FEM. In this approach, the stability of the various elements of the slope was considered as they have varying degrees of influence on the overall stability. The calculation of the factor of safety (Fs) was undertaken using the following equation:

$$Fs = \frac{3c + I_1 \cdot \tan\varphi}{\sqrt{(9 + 12\tan^2\varphi)J_2}} \quad (1)$$

Fig. 10
Measured geological profile I-I′ in Lingquansi cave temple

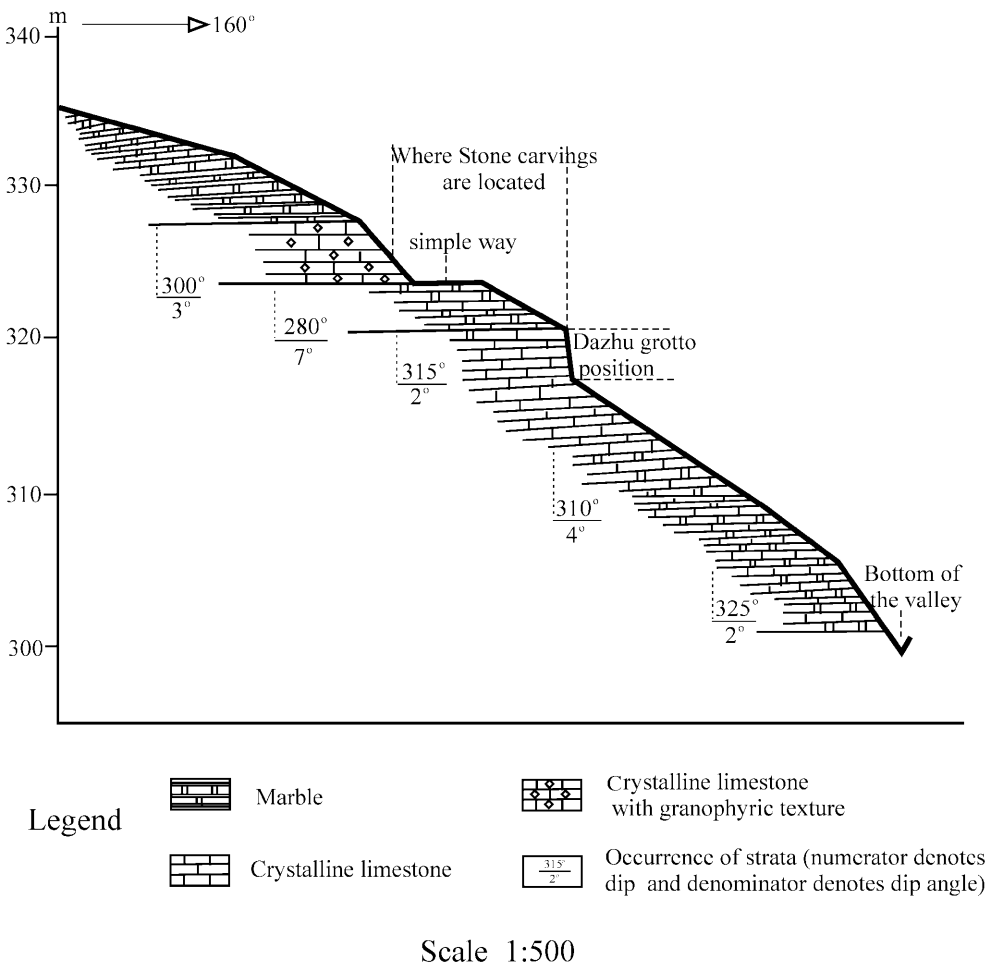

Fig. 11
Simplified geological model and discrete mesh for profile I-I′

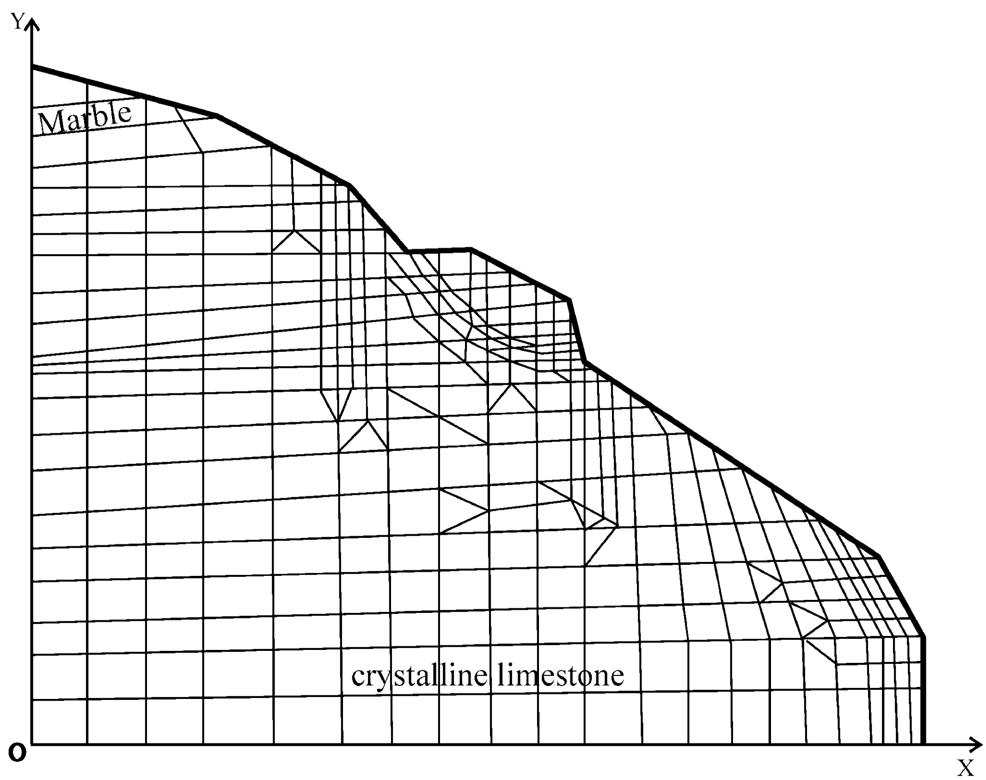

Table 3
Physical/mechanical properties of crystalline limestone and marble

Lithology	Elastic modulus (MPa)	Poisson's ratio	Preliminary cohesive force (MPa)	Preliminary friction angle (°)	Residual cohesive force (MPa)	Residual friction angle (°)	Density (kN/m^3)	Uniaxial tensile strength (MPa)
Marble	10,000	0.25	0.253	32	0.025	22	27.3	0.40
Crystalline limestone	8,000	0.25	0.243	31	0.024	21	27.5	0.20

where I_1 is the first invariant of stress tensor; J_2 is the second invariant of stress deviation.
The analysis showed the factor of safety of every element in the slope is greater than one, hence the slope is presently stable. However, failure conditions could occur under strong seismic activity, so when considering future renovation/conservation measures, this possibility should be taken into account.

Discussion on earthquake influence

The pseudo-static analysis discussed above assumes the earthquake force, varying with time and space, to be a set of horizontal inertia forces, which, at each point of the slope, remain constant with time and are directed horizontally towards the free face (Borg and Schuring 1985; Ashford and Sitar 1995). However, as the horizontal inertial force is not always the most dangerous, the most critical direction of inertial force must be determined. In the case of the grotto, the seismic coefficient Ka is equal to 0.360 (in accordance with an earthquake intensity of 8°). The direction of force (θ) varies from 0 to 360°. Calculations indicate that the most dangerous direction is within a range of 225–315°N, i.e. about 270°N.
Based on the seismic hazard analysis discussed by the Earthquake Society of Henan Province (Anon 1996) and assuming exceeding probability P to be 63, 10 and 3% respectively in a period of 50 years, corresponding horizontal peak accelerations of the bedrock would be 37.9, 113.6 and 223.0 gal and the corresponding seismic coefficient Ka is 0.0387, 0.116 and 0.228. As the cave temple is a long-term conservation objective, in order to guarantee a sufficient margin of safety for future stability in the event of a potentially strong earthquake, predictions should be made on the basis of the most dangerous direction of force.
The results presented in Fig. 12 indicate that seismicity plays a minor role in the overall safety coefficient distribution. However, seismicity is a momentary dynamic event, involving tremor direction (vergence, backward and transverse slide block), tremor times (i.e. fore-quake, main-quake and after-quake effects) and magnitude or acceleration value. Prediction of the effects of earthquakes over a longer period of time therefore represents a problem (Zhenquan 1997). During strong seismic motion, some displacement of the rock mass may occur and possibly be permanent. Sudden instability of the rock mass produces only limited slide displacement and does not necessarily mean that the rock mass loses stability completely. For this reason, earthquake slide displacement may be a better index for strength analysis and design than conventional safety coefficients (Shouyi et al. 1997).

Stability of the blocks

The rock mass structure of the area implies a high level of rock integrity. An important aspect of the study was therefore to determine whether deformation or failure of the discontinuity-bounded blocks could take place. Attention would also be given to weaknesses along the structural planes caused by karst phenomena.
Field observations indicated that the bedding planes are almost horizontal and dip in the opposite direction to the inclination of the slope, thus implying a low probability of block slide along the bedding planes. However, theoretical analysis suggests a comparatively high probability of block toppling failure under seismic activity. Different analytical methods and boundary conditions were used in the calculations for block toppling failure. For simplicity and to ensure a conservative approach, bedding planes dipping gently towards the interior of the slope were considered as horizontal planes.

Single block stability analyses

Single blocks are dissected by three sets of structural planes and are completely separated from the mass. As it is theoretically possible that a single block may both slide and topple, the two aspects are considered separately.

Resistance to sliding

The dynamic condition of a block is presented in Fig. 13. On the assumption that the block does not topple, the safety coefficient K_{RS} of the block resistance to sliding can be defined by the following equation:

$$K_{RS}=\frac{W\cdot\tan\varphi+(s-b)\cdot c}{T+P_w} \qquad (2)$$

where W is the weight of the block; φ and c are the internal friction angle and cohesive force respectively; T is the horizontal earthquake force; P_w is the hydrostatic pressure; s is the length of the sliding plane; and b is the length of the indentation/undercut.

Resistance to toppling

In Fig. 13, point a is the assumed rotation support point. It is apparent that the block has toppled when the length of

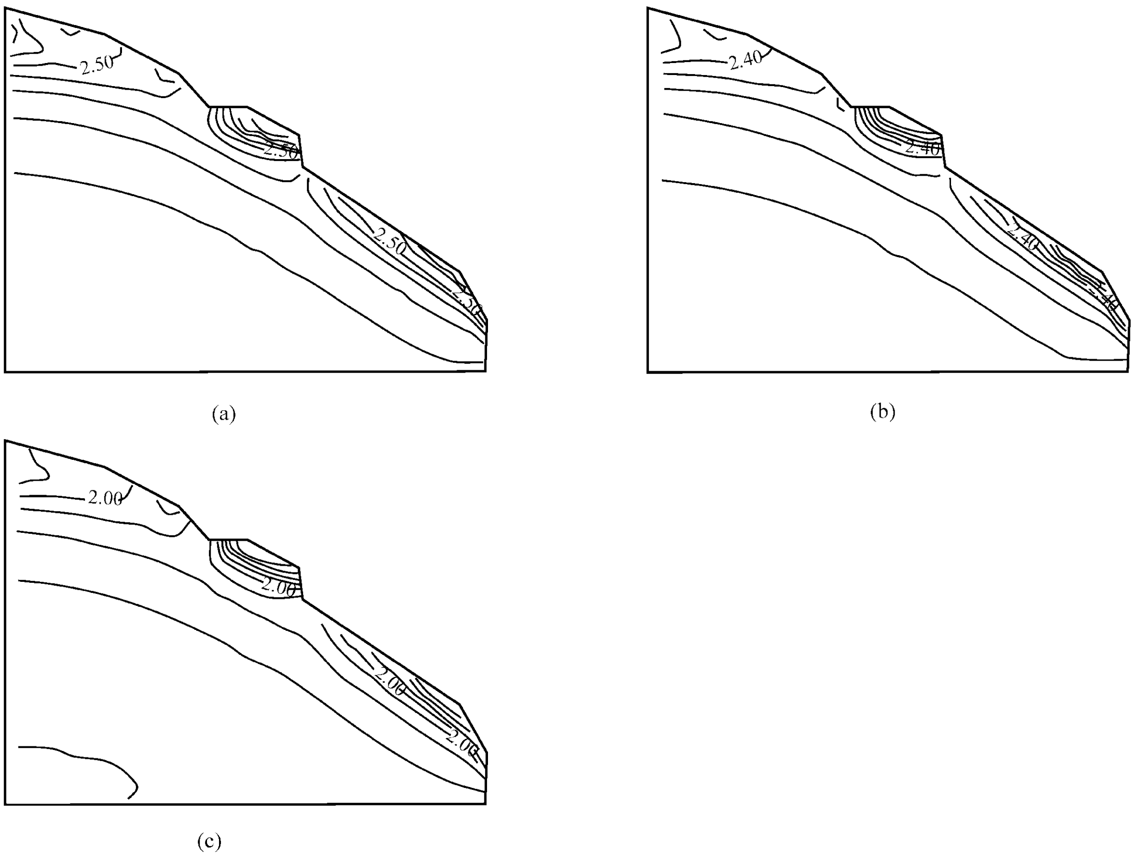

Fig. 12
Isolines for safety factors for different exceeding probabilities. **a** P=63%, Ka=0.0387; **b** P=10%, Ka=0.116; **c** P=3%, Ka=0.228

the indentation b exceeds half the length of the sliding plane $s/2$. In this regard, the analysis of the block resistance to toppling has no significance. When $b<s/2$ the safety coefficient K_{RT} of the block resistance to toppling can be expressed as (Houtian 1989):

$$K_{RT} = \frac{W\cdot(s/2-b)}{T\cdot h/2 + 1/3\,P_w\cdot h_w} \qquad (3)$$

where $(s/2–b)$ is the distance between point a and the plumb line passing the centre of gravity O of the block; $h/2$ is the distance between the centre of gravity O and the bottom boundary; and h_w is the water head.

It should be noted that indentations (undercutting) have been formed at the bottom of certain stone carvings in W5 as mentioned above. Where these stone carvings are located, the stability of the blocks is reduced in terms of both resistance to sliding and resistance to toppling, as shown in Eqs. (2) and (3) respectively. In order to prevent the stone carvings of W5 becoming unstable, therefore, remedial measures should take the weak intercalations at the base of the wall into account.

Influence of groundwater and earthquake forces on stability

A potential toppling block is present in the above-mentioned rock mass, where niches K75 and K76 are located. The crack is wider in the rear of the block and as it is connected with other structural joints, lateral water pressures will not be created. As a consequence, only the effects of earthquake loads were taken into account in the computations for the resistance of this block to toppling. As the earthquake intensity in the study area is 8° and the safety coefficient K_{RT} obtained from Eq. (3) is 2.22, it is not considered very likely that toppling would take place, even under a strong earthquake force.

It should be emphasised, however, that the earthquake force in the above calculation is assumed as an inertia force triggered by the maximum acceleration of ground movements in a planar field. The greater the acceleration, the greater the inertia force. However, the local morphology is one of the main factors affecting local changes in earthquake hazard potential. With strong earthquakes, different parts of a mountain experience different vibration effects. As a rule, the isolated and projecting summit suffers the strongest tremors and the foot of the mountain the least. The intensity of the vibrations affecting the hillside falls between these extremes.

In the study area the stability coefficient calculation indicates that the safety margin is insufficient where the slopes are steep and the average annual rainfall is in the order of 650 mm. The cultural relics will require long-term protec-

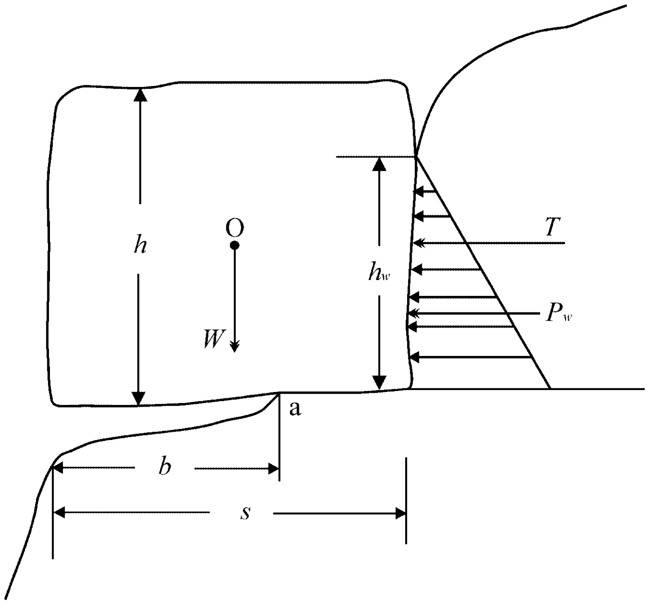

Fig. 13
Stability analysis model for a single block

tion, hence in these areas even low probability events, such as a strong earthquake and intense/prolonged rainfall, must be taken into account in both the stability analyses and any necessary reinforcement/renovation measures.

Multi-block stability analyses

A typical example of a multi-block situation is the dangerous rock mass composed of three disconnected blocks on the eastern escarpment of the grotto (Fig. 4). Each block has the potential to slide toward the free face under earthquake conditions. Each block also has a potential for toppling at some rotation point, prior to such a sliding. It is assumed that there are no moments that would tend to cause sliding of the blocks, hence failure by toppling only is considered. In addition to the intrinsic gravity forces, only a horizontal earthquake force was taken into account. The safety coefficient of each block's resistance to toppling is given by the ratio of the total force resisting toppling to the total force likely to induce toppling. If the safety coefficient is at its critical value (generally unity is used), the displacement value is termed the critical displacement.

For the dangerous rock mass, the actual measured length was 2.4 m, the width at the top 1.4 m and the density 2.7 t/m^3. Each block's rotation point was located before the block moves. The calculations presented in Table 4 indicate that the stability of the upper block is best when the three blocks have not toppled and they are considered separately. Because the gravitational effect of the upper block and the middle block increase the force to induce the bottom block to topple, the stability of the bottom block is worsened. Clearly, therefore, toppling of an upper block assists the stability of other blocks underneath it. When each block is in limiting equilibrium state, the critical displacement value of the bottom block is the lowest (0.39 m)

Renovation recommendations

On the basis of detailed engineering geological studies, the following recommendations and suggestions for comprehensive renovation measures in the Lingquansi Temple are presented.

Table 4
Calculated factor of safety for blocks in the Dazhu Grotto

Calculation plan			Block height (m)	Block displacement (m)	Factor of safety (K)	Critical displacement (m)
Upper block (UB)			0.51	0.30	3.48	
			0.51		1	0.61
Middle block (MB)	Before UB topple	UB	0.51	0.30	1.79	
		MB	0.32	0.20		
	After UB topple	MB	0.32		1	0.64
Lower block (LB)	Before UB and MB topple	UB	0.51	0.30		
		MB	0.32	0.20	1.03	
		LB	1.73	0.10		
	After UB topple	MB	0.32	0.20	1.53	
		LB	1.73	0.10		
	After UB and MB topple	LB	1.73		1	0.39

Renovation of the stone carvings

1. In view of the identification of the different kinds of structural planes and their characteristics, deformation and failure modes in the rock mass escarpment, different remedial measures should be adopted:
   a. Horizontal indentations (undercutting), formed by weathering and corrosion of the weak intercalations at the bottom of the escarpment, should be infilled with schist slurry or concrete.
   b. Rock blocks with a potential for toppling and/or collapse should be bolted to intact and stable bedrock.
   c. Consolidation grouting and other measures should be used to reinforce wider cracks on the escarpment.
   d. Dangerous rock blocks with no cultural value should be removed by hand. Blasting should not be allowed under any circumstances.
2. Control of deterioration due to water percolation, corrosion and weathering could be achieved by:
   a. Pressure grouting with a chemical slurry with good penetration to infill and bond fractures through which seepage can take place.
   b. Construction of a ground surface drainage system in appropriate locations.
3. Earthquakes play a significant role in the stability of the cave temple, which is located in a high earthquake-intensity region. As there are some indeterminable factors in the seismic analyses, it is important that a sufficient margin be adopted when calculating safety coefficients for the renovation measures.
4. Engineering geology and renovation studies should be part of an integrated system comprising many related factors, which contribute to the long-term preservation of this area of cultural importance. It is therefore recommended that high priority be given to monitoring during the planning and implementation of renovation projects (Zhifa et al. 1997). Such monitoring would ensure that works are as cost-effective as possible and the renovation and conservation effects are maximized.
5. Appropriate procedures for the renovation and conservation measures (e.g. reinforcement, grouting, bolting, etc.) should be established prior to the commencement of any works in order to ensure that the original appearance of the stone carvings is preserved.

Renovation of the Dazhu Grotto

The following renovation measures for the Dazhu Grotto are proposed:

1. Potentially unstable blocks intersected by structural planes and free planes are not found in the Dazhu Grotto, hence reinforcement measures such as anchoring and consolidation grouting may only need to be considered in the long term.
2. The following measures for the control of water percolation, corrosion and weathering are recommended:
   a. Pressure grouting with a chemical slurry with good penetration to infill and bond fractures through which seepage can take place.
   b. Construction of a ground surface drainage system in appropriate locations.
3. Appropriate procedures for the renovation and conservation measures (e.g. reinforcement, grouting, bolting, etc.) should be established prior to the commencement of any works in order to ensure that original appearance of the Dazhu Grotto is preserved.

Summary and conclusions

The Lingquansi Cave Temple, which was built 1,450 years ago, is an important national cultural relic. In addition to the ruined temple itself, the site comprises two grottoes and 209 stone carvings. This paper pays particular attention to the Dazhu Grotto and to the stone carvings located on the Bao Mountain's southern escarpment, as they are comparatively better preserved.

Under the influence of natural weathering agents, the grotto and the stone carvings have deteriorated over the centuries. The main problems result from: (1) instability of the rock blocks on the escarpment; (2) water percolation and corrosion; and (3) weathering. Of these, block instability is deemed the most important and in particular the possible toppling or collapse of separated rock blocks.

The problems affecting the grotto are different from those of the stone carvings. For the grotto, deformation of the rock wall, water percolation, corrosion and deposition of carbonate sediments on the surface are principal concerns, while for the stone carvings the main problems are the heavy weathering and corrosion which are defacing the images.

The intersection of structural planes and bedding planes in the rock mass contributes to both the initiation and propagation of the deterioration. In addition, it has been shown that the study area is located in a region of high seismic intensity and that the dislocation of rock blocks is mainly related to earthquakes.

Numerical simulation of the deformation of the slope has been carried out using the computer program FEMA.FOR, in which earthquake force is considered as pseudo-static. Stability calculations based on stress analyses of the rock mass elements suggest that the slope is stable at present and will remain stable in the event of a future strong earthquake as this is likely to have little influence on the safety coefficient distribution. Nevertheless, low probability events such as strong earthquakes and intense rainfall must be taken into account in the stability analyses in order to guarantee a sufficient safety margin for both the renovation and future preservation of this historic area.

The problems mentioned above have caused different kinds of damage in the grotto and the stone carvings. For sustainable preservation and protection it is imperative that comprehensive renovation is undertaken. Appropriate measures are put forward and attention is drawn to the importance of ensuring that renovation and conservation measures do not damage the original appearance of the grotto and the stone carvings.

It is strongly recommended that engineering geological monitoring should be carried out on a continued basis. In addition, further studies of the seismic factors are proposed, as the prediction of multi-earthquake effects is a complex problem. Earthquake slide displacement may be the most appropriate index for stability analyses and renovation designs for the slope. Not only the characteristics of earthquake forces but also the inherent dynamic characteristics of the rock mass must be considered when assessing and evaluating the effect of earthquakes on its stability.

Acknowledgments The authors are grateful to Mr. Tue Jensen (Denmark) for reading the manuscript and for discussion and valuable comments. The authors also acknowledge financial support from the National Natural Science Foundation (no. 49772166) and from the Engineering Geo-mechanism Open Research Laboratory, Institute of Geology and Geophysics of the Chinese Academy of Sciences.

References

Anon (1991) Bao Mountain of Lingquansi Cave Temple. Henan Provincial Institute of Ancient Architecture Preserve (ed). Henan People Press, Henan, pp 1–10

Anon (1996) Evaluation report on seismic safety for engineering field of building complex for Bank of Agriculture in Linzhou City. Earthquake Society of Henan Province, Henan

Ashford SA, Sitar N (1995) Seismic coefficients for steep slopes. Soil Dynamics and earthquake Engineering, Computational Mechanics Publications, Southampton, pp 441–447

Bietong P, Kezhong H (1992) The culture relic conservancy and environmental geology. China University of Geosciences Press, Wuhan

Bietong P, Runqiu H (1994) Numeric methods of engineering geology. Geology Press, Beijing

Borg SF, Schuring JR (1985) A rational method for analyzing rock slope stability due to an Earthquake. Soil Dynamics and Earthquake Engineering, Computational Mechanics Publications, Southampton, pp 517–526

Dezhen G (1979) The fundamental of rock engineering geomechanics. Science Press, Beijing, pp 206–207, 232–233

Handong L (1997) Stability study of the high slope rock mass in the workshop of Xiaoshan water and electric station. J Eng Geol 5:218–223

Houtian H (1989) Collapse and falling. Railway Press of China, Beijing, pp 58–70

Shouyi X, Sijing W, Jianzhong L (1997) Earthquake slide displacement analyses of the block rockmass slope. J Eng Geol 5:131–136

Xinpu S, Bingye X, Zhangzhi C (1995) Computational rock mechanics – theory and practice. China Environment Science Press, Beijing

Yunfei H, Jing F (1992) Computational engineering geology (theory,·programs,·examples). Engine of War Industry Press, Beijing, pp 159–170

Zhenquan C (1997) Deformation and instability forecast of the bank slope (special report). In: Proc 4th Natl Youth Engineering Geology Symp, Engineering Geology – Face the 21st Century, China University of Geosciences Press, Wuhan, pp 595–601

Zhifa Y, Da'an L, Ying L, Yanjun S, Baoyuan Y (1997) Plan for slope monitoring system and analysis methods of monitoring information. In: Proc Natl Symp on the Ground and Foundation in Mountainous Areas, Chongqing, pp 1–13